JOURNAL OF SOLID STATE CHEMISTRY 92, 110–115 (1991)

Anionic Vacancy Distribution in Reduced Barium–Lanthanum Ferrites: $Ba_xLa_{1-x}FeO_{3-x/2}$ ($1/2 \leq x \leq 2/3$)

J. M. GONZÁLEZ-CALBET AND M. PARRAS

Departamento de Química Inorgánica, Facultad de Ciencias Químicas, Universidad Complutense, 28040-Madrid, Spain

M. VALLET-REGÍ

Departamento de Química Inorgánica y Bioinorgánica, Facultad de Farmacia, Universidad Complutense, 28040-Madrid, Spain

AND J. C. GRENIER

Laboratoire de Chimie du Solide du C.N.R.S., Université de Bordeaux I, 33405 Talence-Cedex, France

Received September 21, 1990; in revised form December 7, 1990

An electron diffraction and microscopy study of the $Ba_xLa_{1-x}FeO_{3-x/2}$ ($\frac{1}{2} \leq x \leq \frac{2}{3}$) system shows these samples to be formed by three-dimensional microdomains. The unit cell corresponding to each domain is related to the cubic perovskite structure by the expression $a_c \times a_c \times 2a_c$, a_c being the cubic perovskite unit cell parameter. A structural model in which octahedral and square pyramidal layers intergrow in an ordered way following the double axis is proposed. © 1991 Academic Press, Inc.

Introduction

Several studies devoted to compositional variations in perovskite-related materials have shown that the intergrowth of two or more basic structural motifs in various proportions can originate new materials, as observed in phases intermediate between the perovskite and the brownmillerite ($Ca_2Fe_2O_5$) structural types (*1–4*).

In these materials, perovskite-like octahedra layers form an intergrowth with tetrahedra layers in ordered sequences whose general formula is $A_nM_nO_{3n-1}$. Between brownmillerite ($n = 2$) and perovskite ($n = \infty$), two more ordered terms have been isolated up to now:

—$n = 3$, with $AMO_{2.67}$ composition, in $Ca_2LaFe_3O_8$, whose stacking sequence is . . .OOTOOT. . . (O = octahedra, T = tetrahedra) (*5*).

—$n = 4$, i.e., the $AMO_{2.75}$ material ($Ca_4Fe_2Ti_2O_{11}$), in which three octahedral layers alternate with one tetrahedral layer, following the . . .OOOTOOOT'. . . stacking sequence due to the relative orientation of the tetrahedra along the *b* axis (*6*).

In a previous paper (*7*), we have undertaken a study of the system formed between

0022-4596/91 $3.00

TABLE I
CHEMICAL ANALYSIS AND UNIT CELL PARAMETERS OF $Ba_xLa_{1-x}FeO_{3-y}$ MATERIALS

	x	% Fe^{4+}	Nominal composition	a_c(Å)
Oxidized samples	$\frac{1}{2}$	41	$Ba_{\frac{1}{2}}La_{\frac{1}{2}}FeO_{2.94}$	3.942
	$\frac{2}{3}$	38	$Ba_{\frac{2}{3}}La_{\frac{1}{3}}FeO_{2.85}$	3.948
Reduced samples	$\frac{1}{2}$	0	$Ba_{\frac{1}{2}}La_{\frac{1}{2}}FeO_{2.75}$	3.956
	$\frac{2}{3}$	0	$Ba_{\frac{2}{3}}La_{\frac{1}{3}}FeO_{2.67}$	3.981

$LaFeO_3$ and $Ba_2Fe_2O_5$. When $Ba_xLa_{1-x}FeO_{3-y}$ materials are fired in air, a mixed oxidation state of iron (Fe^{4+}, Fe^{3+}) is obtained, compositional variations being accommodated in a different way than in other perovskite-related ferrites (*8, 9*). This is probably due to the bigger size of barium, which is probably responsible for the original way of the oxygen vacancy ordering observed in $Ba_2Fe_2O_5$; its structure has a unit cell different from the brownmillerite structure of $Ca_2Fe_2O_5$, although their parameters are still multiples of the cubic perovskite cell (*10, 11*).

We describe in this paper the microstructural aspects of the $Ba_xLa_{1-x}FeO_{3-x/2}$ ($\frac{1}{2} \leq x \leq \frac{2}{3}$) samples prepared under reducing conditions, i.e., when all iron is in the III oxidation state.

Experimental

Oxidized $Ba_xLa_{1-x}Fe^{3+,4+}O_{3-y}$ samples, prepared as described in Ref. (*7*) were annealed at 1100°C for 24 hr, in flowing Ar–5% H_2. Chemical analysis [also described in Ref. (*7*)] indicates that all iron is found in the III oxidation state. Table I shows the chemical composition of both oxidized and reduced samples for $x = \frac{1}{2}$ and $x = \frac{2}{3}$.

Powder X-ray diffraction was performed on a Siemens D-500 diffractometer equipped with a secondary graphite monocromator and using Cu$K\alpha$ radiation.

Electron diffraction was carried out on a JEOL 2000FX electron microscope, fitted with a double tilting goniometer stage (±45°). High resolution electron microscopy was performed on a JEOL 4000 EX electron microscope fitted with a double-tilting goniometer stage (± 25°), by working at 400 Kv. The samples were ultrasonically dispersed in *n*-butanol and transferred to carbon-coated copper grids.

Results and Discussion

Powder X-ray diffraction data can be indexed on the basis of a cubic single perovskite unit cell as previously observed in oxidized samples. Unit cell parameters are listed in Table I. It can be seen that in both series of samples the cubic parameter increases as a function of the barium content, due to the bigger size of this cation. Nevertheless, the smaller size of Fe^{4+} with respect to Fe^{3+} seems to be responsible for the expansion observed in the unit cell parameter of the reduced samples.

This unit cell is confirmed by electron diffraction for the oxidized samples, which indicates that the small concentration of anionic vacancies ($y \leq 0.15$) is randomly distributed along the crystal. However, electron diffraction and microscopy results corresponding to the reduced samples show a more complex situation.

Figure 1 shows the electron diffraction pattern (EDP) of the $x = \frac{1}{2}$ sample along the $[001]_c$ zone axis, indexed on the basis of a single cubic perovskite. Very weak extra spots are doubling both a^* and b^* axes, but no extra reflexions are seen on the $(\frac{1}{2}\ \frac{1}{2}\ 0)^*_c$ and equivalent positions.

By tilting 45° around the a^* axis, the $[0\bar{1}1]_c$ zone axis is observed (Fig. 2), where only the a^* direction is doubled. In fact, if both a^* and b^* axes were doubled, extra spots on $(\frac{1}{2}\ \frac{1}{2}\ 0)^*_c$ and $(\frac{1}{2}\ \frac{1}{2}\ \frac{1}{2})^*_c$ and equivalent reflexions should appear.

The $[0\bar{1}2]_c$ zone axis is seen in Fig. 3, showing again doubling along the a^* direc-

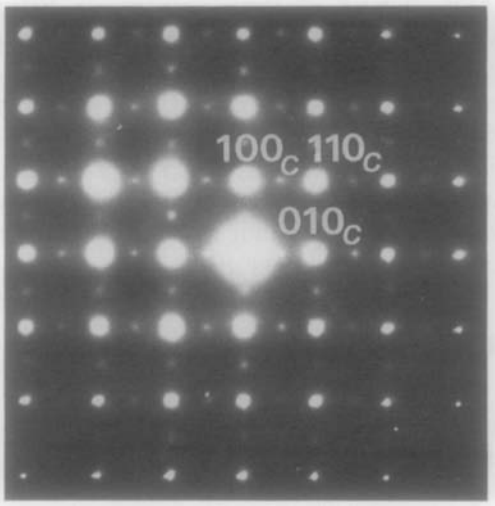

FIG. 1. EDP of $Ba_{\frac{1}{2}}La_{\frac{1}{2}}FeO_{2.75}$ along the $[001]_c$ zone axis.

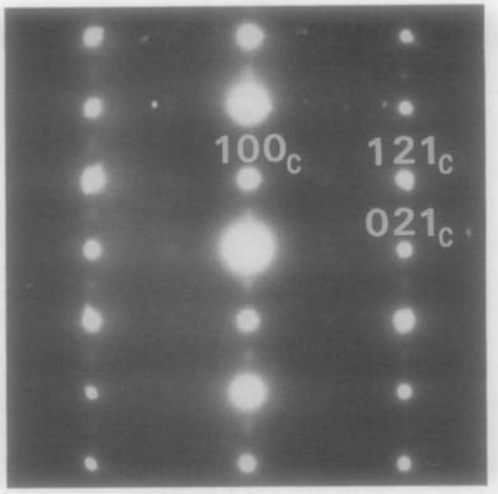

FIG. 3. EDP corresponding to $x = \frac{1}{2}$ along $[0\bar{1}2]_c$ zone axis.

tion but also doubling following $(021)^*_c$ and equivalent directions, which suggests doubling of the c^* axis.

The EDP along the $[0\bar{1}3]_c$ zone axis (Fig. 4) shows again doubling of the a^* axis, but no extra spots are seen on $(0\ \frac{3}{2}\ \frac{1}{2})^*_c$ and $(\frac{1}{2}\ \frac{3}{2}\ \frac{1}{2})^*_c$ and equivalent reflexions.

The above results suggest that, although the three perovskite axes seem to be doubled, the unit cell does not correspond to a double cubic cell. A schematic representation of the above EDP within a reciprocal net corresponding to the perovskite substructure is shown in Fig. 5. According to that, the true reciprocal lattice of $Ba_{\frac{1}{2}}$

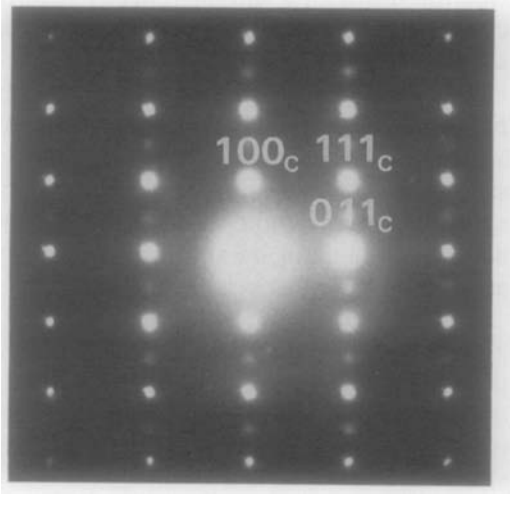

FIG. 2. EDP of the $x = \frac{1}{2}$ material along the $[0\bar{1}1]_c$ zone axis.

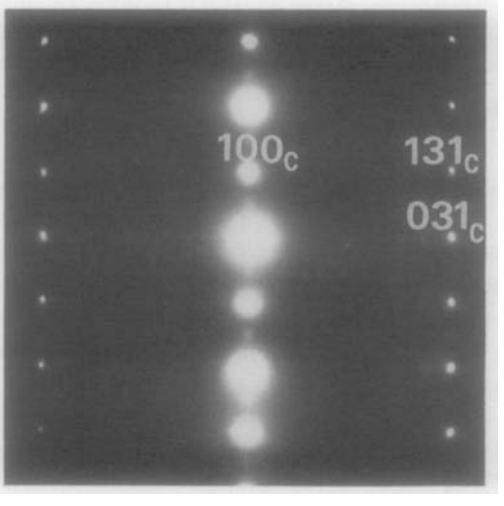

FIG. 4. EDP corresponding to $x = \frac{1}{2}$ along the $[0\bar{1}3]$ zone axis.

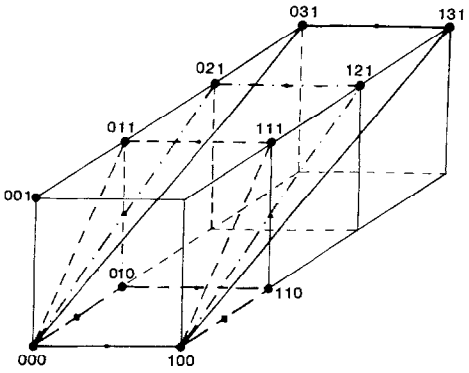

FIG. 5. Schematic representation of the different reciprocal planes recorded by electron diffraction within a reciprocal net corresponding to the cubic perovskite sublattice.

$La_{\frac{1}{2}}FeO_{2.75}$ is formed by the juxtaposition of three reciprocal spaces (Fig. 6a), each of them corresponding to one set of domains whose double axis is randomly distributed along the three space directions: Set A for the domains having the double axis parallel to a_c^* (Fig. 6b), set B for those domains having unit cell parameters $a_c \times 2a_c \times a_c$ (Fig. 6c), and set C for the microdomain set with $a_c \times a_c \times 2a_c$ (Fig. 6d).

The presence of these kinds of microdomains, previously observed in the $Sr_xNd_{1-x}FeO_{3-y}$ system (*12*), is confirmed by high resolution electron microscopy (Fig. 7). The image along the $[001]_c$ direction reveals the existence of a microdomain texture formed by three sets of domains: Domain A and B are clearly rotated 90° as can be seen following both [110] directions (marked by dark arrows). Image contrast shows lattice fringes at 7.8 Å but electron diffraction patterns indicate that only one axis is doubled in each domain. Finally, domain C, where perpendicular fringes of 3.9 Å can be observed, indicating that the double axis is in the c direction.

These reduced samples have been studied by Gibb and Matsuo (*13*) by means of Mössbauer spectroscopy. According to these authors no evidence of tetrahedral sites was

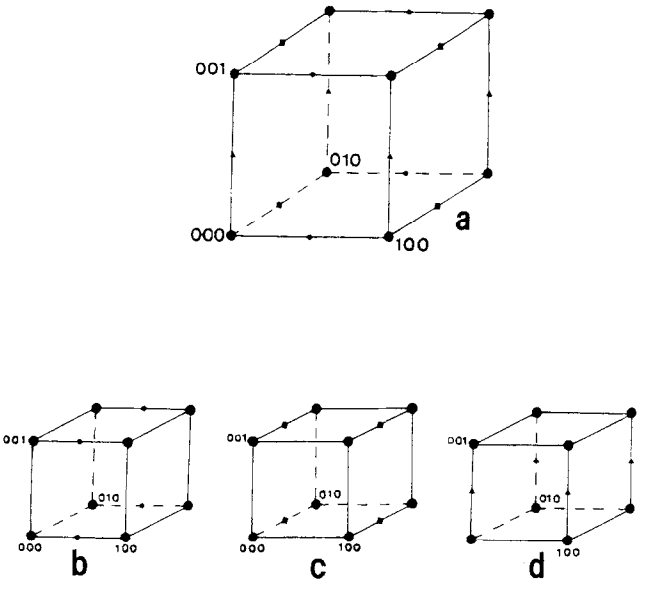

FIG. 6. (a) Complete reciprocal lattice of $Ba_{\frac{1}{2}}La_{\frac{1}{2}}FeO_{2.75}$ composed by the juxtaposition of the three reciprocal nets shown in (b) $2a_c x\ a_c x\ a_c$; (c) $a_c x\ 2a_c x\ a_c$; and (d) $a_c x\ a_c x\ 2a_c$.

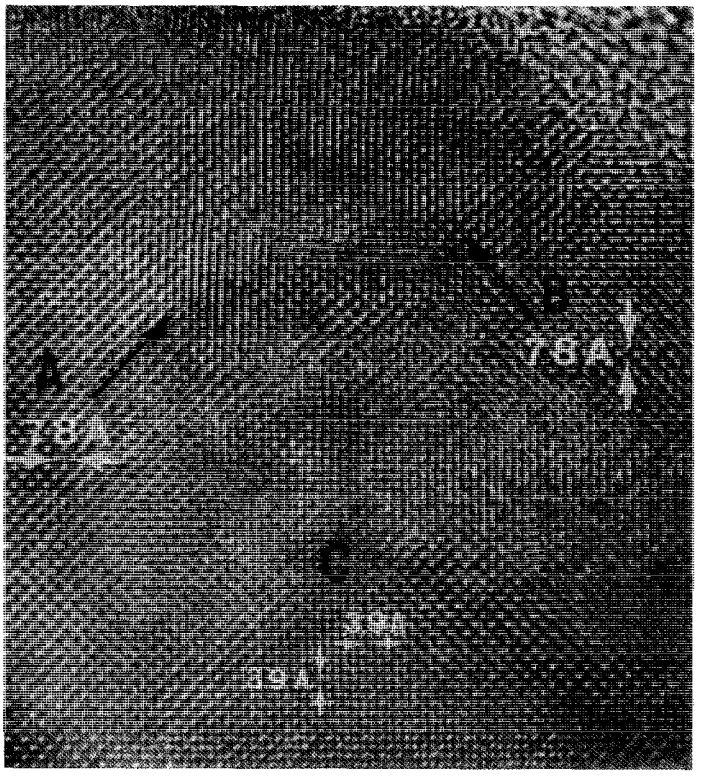

FIG. 7. HREM of $Ba_{\frac{1}{2}}La_{\frac{1}{2}}FeO_{2.75}$ taken with $[001]_c$ beam incidence showing a microdomain texture.

observed for $x = 0.5$. At this point, it is worth mentioning that in the $Ca_xLa_{1-x}FeO_{3-x/2}$ system only octahedra and tetrahedra sites were detected by Mössbauer spectroscopy (*14*), where 25% of tetrahedra sites were observed for $x = 0.50$ composition. However, Gibb and Matsuo (*15*) concluded that the behavior for the $Ba_xLa_{1-x}FeO_{3-x/2}$ system is similar to that observed for the cubic phases of $Sr_2MFe_3O_8$ (*13*), the vacancy ordering to give tetrahedral sites becoming less favorable with increasing the lanthanum content in the Ba/La system. Thus, the concentration of anionic vacancies for $x = 0.5$, i.e., $y = 0.25$, produces around 50% of the five-fold coordinated sites.

A stacking sequence of 50% octahedra and 50% square pyramidal sites, as deduced from Mössbauer spectroscopy results, correspond to an $AMO_{2.75}$ composition. If, as observed in the electron diffraction patterns, only one axis is doubled within each domain, an ordered model of octahedral layers alternating along one axis with square pyramidal layers can be proposed for $Ba_{\frac{1}{2}}La_{\frac{1}{2}}FeO_{2.75}$. However, if the ordering of anionic vacancies is as in the structural model shown in Fig. 8, at least two axes should be double to justify the unit cell.

Since only one axis seems to be double inside each domain, the most likely model for this sample is that in which one octahedral layer alternates in an ordered way with one $FeO_{2.5}\square_{0.5}$ layer in which iron shows square pyramidal coordination but oxygen vacancies are disordered along the *ab* plane (Fig. 9), giving the unit cell parameter $a_c \times$

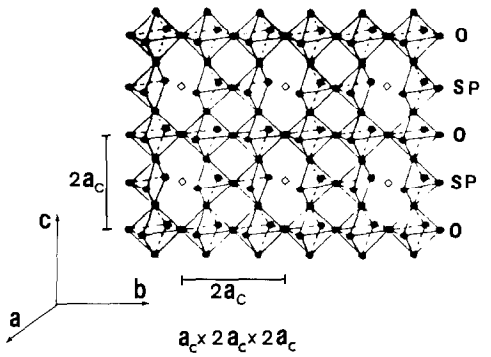

FIG. 8. Structural model for $Ba_{\frac{1}{2}}La_{\frac{1}{2}}FeO_{2.75}$ showing ordering of anionic vacancies.

$a_c \times 2a_c$. If this kind of disorder alternates at random in different parts of crystals along both the *ac* and the *bc* planes, a three-dimensional microdomain texture solid, exhibiting the reciprocal lattice proposed in Fig. 5a, is obtained.

Similar EDP were obtained for the $x = \frac{2}{3}$ reduced sample. According to the structural model proposed for the $A_nM_nO_{3n-1}$ series when $n = 3$ and sites A are occupied by Ca and La, the concentration of tetrahedral sites is 33%. However, Gibb and Matsuo (*13*) only found some 18% tetrahedra in the Ba/La sample with $x = \frac{2}{3}$, while 54% sites

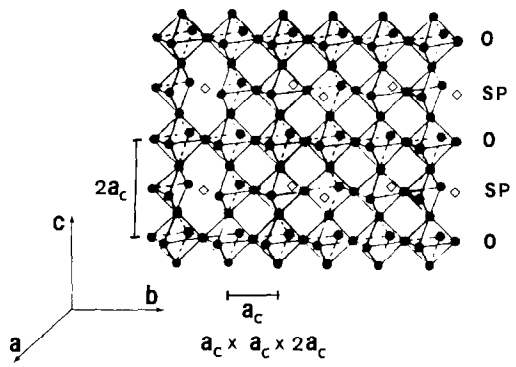

FIG. 9. Structural model proposed for a domain showing $Ba_{\frac{1}{2}}La_{\frac{1}{2}}FeO_{2.75}$ composition and anionic vacancies disordered along the *ab* plane.

were in octahedral position and 28% in pyramidal coordination, leading also to the $AMO_{2.67}$ composition. Regarding these results and taking into account that electron diffraction pattern shows random distribution of a double perovskite axis, the same structural model shown in Fig. 9 can be assumed for this sample if random distribution of tetrahedral sites is included.

Acknowledgment

We thank the CICYT (Programa de Nuevos Materiales) for financial support (Research Project No MAT88-0163-CO3-03).

References

1. J. C. GRENIER, M. POUCHARD, AND P. HAGENMULLER, *Struct. Bonding* **47,** 1 (1981).
2. Y. BANDO, Y. SEKIKAWA, H. YAMAMURA, AND Y. MATSUI, *Acta Crystallogr. Sect. A* **37,** 723 (1981).
3. N. NGUYEN, Y. CALOGE, F. VARRET, G. FEREY, V. CAIGNAERT, M. HERVIEU, AND B. RAVEAU, *J. Solid State Chem.* **53,** 398 (1984).
4. J. M. GONZÁLEZ-CALBET, J. ALONSO, AND M. VALLET-REGÍ, *J. Solid State Chem.* **71,** 331 (1987).
5. J. C. GRENIER, F. MÉNIL, M. POUCHARD, AND P. HAGENMULLER, *Mater. Res. Bull.* **12,** 79 (1977).
6. J. M. GONZÁLEZ-CALBET AND M. VALLET-REGÍ, *J. Solid State Chem.* **68,** 266 (1987).
7. M. PARRAS, M. VALLET-REGÍ, J. M. GONZÁLEZ-CALBET, M. ALARIO-FRANCO, AND J. C. GRENIER. *J. Solid State Chem.* **74,** 110 (1988).
8. M. A. ALARIO-FRANCO, J. M. GONZÁLEZ-CALBET, M. VALLET-REGÍ, AND J. C. GRENIER, *J. Solid State Chem.* **49,** 219 (1983).
9. J. M. GONZÁLEZ-CALBET, M. VALLET-REGÍ, AND M. A. ALARIO-FRANCO, *J. Solid State Chem.* **60,** 320 (1985).
10. M. PARRAS, M. VALLET-REGÍ, J. M. GONZÁLEZ-CALBET, M. A. ALARIO-FRANCO, J. C. GRENIER, AND P. HAGENMULLER, *Mater. Res. Bull.* **22** (1987) 1413.
11. X. D. ZOU, S. HÖVMOLLER, M. PARRAS, M. VALLET-REGÍ, J. M. GONZÁLEZ-CALBET, AND J. C. GRENIER, to be published.
12. M. A. ALARIO-FRANCO, J. C. JOUBERT, AND J. P. LEVY, *Mater. Res. Bull.* **17,** 733 (1982).
13. T. C. GIBB AND M. MATSUO, *J. Solid State Chem.* **81,** 83 (1989).
14. J. C. GRENIER, L. FOURNES, M. POUCHARD, P. HAGENMULLER, AND S. KOMORNICKI, *Mater. Res. Bull.* **17,** 55 (1982).
15. P. D. BATTLE, T. C. GIBB AND S. NIXON, *J. Solid State Chem.* **79,** 86 (1989).